*applied sciences*

MDPI

*Article*

# Protective Effects of the Ethyl Acetate Fraction of *Distylium racemosum* Against Metabolic Dysfunction-Associated Steatohepatitis

**Young-Hyeon Lee [1], Min-Ho Yeo [1], Kyung-Soo Chang [1], Weon-Jong Yoon [2], Hye-Sook Kim [3], Jongwan Kim [4,*,†] and Hye-Ran Kim [5,*,†]**

[1] Department of Clinical Laboratory Science, Catholic University of Pusan, Busan 46252, Republic of Korea
[2] Clean Bio Business Division, Biodiversity Research Institute (JBRI), Jeju Technopark (JTP), Seogwipo 63608, Republic of Korea
[3] Department of International Infectious Diseases Control, Faculty of Medicine, Dentistry and Pharmaceutical Sciences, Okayama University, Tsushima-Naka, Kita-Ku, Okayama 700-8530, Japan; hskim@cc.okayama-u.ac.jp
[4] Department of Anatomy, College of Medicine, Dongguk University, Gyeongju 38066, Republic of Korea
[5] Department of Biomedical Laboratory Science, Dong-Eui Institute of Technology, Busan 47230, Republic of Korea
* Correspondence: dahyun@dongguk.ac.kr (J.K.); hrkim@dit.ac.kr (H.-R.K.); Tel.: +82-54-770-2414 (J.K.); +82-51-860-3521 (H.-R.K.)
† These authors contributed equally to this work.

## Abstract

Metabolic dysfunction-associated steatohepatitis (MASH), previously referred to as non-alcoholic steatohepatitis (NASH), which is a progressive non-alcoholic fatty liver disease, is accompanied by hepatic steatosis, inflammation, and fibrosis. Despite its increasing prevalence, available treatment options for MASH are limited. Here, we investigated the protective effects of the *Distylium racemosum* ethyl acetate fraction (DRE) using MASH models and explored its key physiologically active components. Palmitic acid (PA)-induced AML12 hepatocytes and high-fat methionine- and choline-deficient-fed C57BL/6 mice were used as MASH models. Lipid accumulation was evaluated via triglyceride measurement, oil red O staining, and histological analysis. Lipid accumulation, inflammation, and fibrosis-associated gene expression were evaluated via real-time polymerase chain reaction. The physiologically active components of DRE were identified via high-performance liquid chromatography. Lipid accumulation and triglyceride levels were significantly reduced in PA-treated AML12 cells following DRE treatment. Additionally, DRE inhibited the expression of genes involved in lipogenesis (*FAS* and *SREBP1c*), inflammation *(CD68*, *IL-6*, and *MCP-1*), and fibrosis (*COL1A1*, *COL1A2*, and *TIMP1*). DRE reduced the liver weight, liver-to-body weight ratio, and hepatic steatosis in MASH model mice. It increased carnitine palmitoyltransferase-1 levels and decreased *CD36* and transforming growth factor-β levels in the MASH mouse liver. High-performance liquid chromatography revealed that the extract contained rutin flavonoid family members. Overall, DRE was involved in lipid metabolism, inflammation, and fibrosis regulation, exerting potent hepatoprotective effects partly attributed to rutin and serving as a potential preventive candidate for MASH.

**Keywords:** metabolic dysfunction-associated steatohepatitis; *Distylium racemosum*; ethyl acetate fraction; extract



Academic Editor: Francisco Arrebola

Received: 27 May 2025
Revised: 25 June 2025
Accepted: 25 June 2025
Published: 27 June 2025

**Citation:** Lee, Y.-H.; Yeo, M.-H.; Chang, K.-S.; Yoon, W.-J.; Kim, H.-S.; Kim, J.; Kim, H.-R. Protective Effects of the Ethyl Acetate Fraction of *Distylium racemosum* Against Metabolic Dysfunction-Associated Steatohepatitis. *Appl. Sci.* **2025**, *15*, 7238. https://doi.org/10.3390/app15137238

## 1. Introduction

Metabolic dysfunction-associated steatotic liver disease (MASLD), previously termed non-alcoholic fatty liver disease (NAFLD), represents a spectrum of hepatic disorders characterized by excessive triglyceride (TG) accumulation in hepatocytes in the absence of significant alcohol consumption. MASLD encompasses simple steatosis, which is generally benign, as well as its progressive form, metabolic dysfunction-associated steatohepatitis (MASH, formerly known as NASH), which is marked by inflammation, hepatocellular injury, and varying degrees of fibrosis.

In advanced stages, MASH can progress to cirrhosis, liver failure, and hepatocellular carcinoma [1–3]. Unlike simple steatosis, MASH is pathologically characterized by hepatocyte ballooning, cell death, and infiltration of inflammatory cells [4–6]. It is estimated that approximately 25% of patients with MASLD develop MASH, and nearly 20% of those with MASH eventually progress to cirrhosis or liver cancer, particularly in the context of obesity.

In accordance with a recent consensus by international liver disease societies, the term "non-alcoholic steatohepatitis (NASH)" has been updated to "MASH" to better reflect its metabolic etiology and to reduce the stigma associated with alcohol consumption [7]. This nomenclature shift, along with the proposed transition from NAFLD to MASLD, provides a more inclusive and mechanism-based framework for disease classification, diagnosis, and management.

The progression to MASH is widely explained by the two-hit hypothesis. The first hit is associated with lipid accumulation, following insulin resistance, obesity, and de novo adipogenesis. The second hit results in fibrosis of the liver tissue and chronic liver injury via oxidative stress, pro-inflammatory cytokine production, and apoptosis [8]. Despite its increasing global prevalence, only limited prevention and treatment options are currently available for MASH.

Natural product-derived compounds have attracted attention as potential preventive and therapeutic agents owing to their antioxidant, anti-inflammatory, and inhibitory effects on lipid accumulation. Some nutraceuticals, including silymarin, curcumin, and resveratrol, have shown promising hepatoprotective effects against MASH by modulating oxidative stress, inflammation, and lipid metabolism. However, these examples are relatively few, and the discovery of novel natural compounds targeting MASH remains limited, indicating the need for further exploration [9]. *Distylium racemosum* (*D. racemosum*), an evergreen plant native to Jeju Island, exerts various effects, such as anti-obesity, antioxidant, and anti-inflammatory [10]. However, its hepatoprotective effects and molecular mechanisms against MASH remain unknown.

Individuals with MASH show a substantially increased likelihood of liver cancer development compared to those with viral hepatitis, particularly in the presence of obesity [11]. This highlights the urgent need for effective treatment methods for MASH. As the *D. racemosum* ethyl acetate fraction (DRE) exerts anti-obesity effects, its active ingredient possibly protects against MASH.

In this study, we investigated the effects and action mechanisms of DRE on MASH using hepatocytes and mouse models. We also evaluated the potential of DRE as a MASH prevention and treatment agent by analyzing its key active ingredients via high-performance liquid chromatography (HPLC) analysis.

## 2. Materials and Methods

### 2.1. Preparation of D. racemosum Fractions

Leaves of *D. racemosum* native to Jeju Island were washed with distilled water and dried to remove moisture. The dried leaf samples were ground into powder and extracted twice with 70% ethanol. The resulting extracts were filtered, concentrated under reduced

pressure, and completely dried using a freeze dryer. The dried ethanol extract was then suspended in ten times its volume of distilled water and partitioned sequentially with an equal volume of n-hexane, ethyl acetate, and n-butanol to obtain the respective fractions. Each solvent fraction was collected after concentration under reduced pressure. All fractionation steps were performed in duplicate to ensure reproducibility. The final extracted materials were prepared at a concentration of 10 mg/mL for use in subsequent experiments.

### 2.2. Cell Viability Assay

To determine the optimal concentration of palmitic acid (PA) for fatty liver induction in alpha mouse liver 12 (AML12) cells (American Type Culture Collection, Manassas, VA, USA), the cells were treated with various concentrations of PA (0.25–0.5 mM) (ChemFaces, Wuhan, China). After induction, the 3-(4,5-dimethyl-2-thiazolyl)-2,5-diphenyltetrazolium bromide assay was performed to determine the appropriate concentration of the test substance. AML12 cells were seeded in a 96-well microplate at a density of $1 \times 10^5$ cells/well and incubated for 24 h. The following day, the cells were treated with DRE at concentrations of 0, 25, 50, and 100 μg/mL for 24 h. After treatment, the cells were incubated with the 3-(4,5-dimethyl-2-thiazolyl)-2,5-diphenyltetrazolium bromide solution, and the resulting formazan crystals were dissolved in dimethyl sulfoxide. Absorbance was measured at 540 nm to assess the cell viability.

### 2.3. Lipid Accumulation Analysis

To quantify the intracellular TG levels, the cells were lysed and lipids were extracted using a commercial neutral lipid quantification reagent set (Asan Pharmaceutical, Seoul, Republic of Korea). TG levels were measured according to the manufacturer's instructions [12]. Lipid accumulation was visualized via oil red O (Sigma-Aldrich, St. Louis, MO, USA) staining to qualitatively assess the degree of steatosis.

### 2.4. Real-Time Quantitative Polymerase Chain Reaction

DRE-treated cells were washed with phosphate-buffered saline, and total RNA was extracted using an RNA isolation kit (Bioneer, Daejeon, Republic of Korea). RNA purity and concentration were evaluated, and cDNA was obtained using a cDNA synthesis kit GoScript™ reverse transcription system, Promega, USA). A real-time polymerase chain reaction was performed using the SYBR-Green Master Mix (Applied Biosystems, Foster City, CA, USA). Gene-specific primers were designed to target the key genes involved in lipid synthesis, inflammation, and fibrosis [13]. Relative gene expression levels were calculated using the ΔΔCt method.

### 2.5. MASH Model Induction via a High-Fat Methionine- and Choline-Deficient (HFMCD) Diet

To establish a murine model of MASH, six-week-old C57BL/6 mice were acclimatized for one week and randomly assigned to four groups (n = 8/group) based on body weight. The control group was fed a standard normal diet (ND), whereas the experimental groups were fed an HFMCD diet containing 60% fat and 0.1% methionine with no added choline to induce MASH. Food and water were provided ad libitum, and body weights were recorded every two days. All animal procedures were approved by and adhered to the guidelines of the Institutional Animal Care and Use Committee of the Catholic University of Pusan (approval no. CUP AEC 2023-002).

### 2.6. Tissue Collection and Histological Analysis

After fasting for 13 h, the mice were euthanized using $CO_2$. Their liver tissues were collected, washed with sterile phosphate-buffered saline, and moisture was removed to measure the weight. The liver tissues were fixed with 4% formalin, and dehydrated tissues

were embedded in paraffin and sliced into 4-μm-thick sections. The section slides were prepared to stain the samples with hematoxylin and eosin (H&E).

### 2.7. HPLC Profiling of the Active Components

Active constituents of DRE were analyzed via high-performance liquid chromatography (HPLC). Separation was performed using a 2.1 × 100 mm HSS T3 column with 1.8 μm particle size (Waters), maintained at 40 °C. The mobile phase consisted of Solvent A (distilled water with 0.1% formic acid) and Solvent B (acetonitrile). A gradient elution program was applied with a flow rate of 0.3 mL/min. The injection volume ranged from 2 to 6 μL. Detection was carried out using a UV-Vis detector at 360 nm.

### 2.8. Statistical Analyses

Data are represented as the mean ± standard deviation. All data were analyzed via the one-way analysis of variance, and mean differences were analyzed via the Tukey–Kramer post hoc test. Statistical significance was set at $p < 0.05$.

## 3. Results

### 3.1. Effects of DRE on Cell Viability and Lipid Accumulation in PA-Induced AML12 Cells

To evaluate the cytotoxicity of and lipid accumulation inhibition by DRE, AML12 cells were treated with PA in the presence or absence of DRE. Cell viability was not significantly affected by either DRE concentrations, indicating the safety of DRE under the tested experimental conditions (Figure 1A). PA significantly increased the intracellular TG levels compared to those in the control group (Figure 1B). However, co-treatment with DRE at 25 and 50 μg/mL significantly reduced TG accumulation in a dose-dependent manner. Oil red O staining revealed markedly increased lipid accumulation in the PA-treated cells, which was significantly attenuated by DRE (Figure 1C). This attenuation was more pronounced at high DRE concentrations (50 μg/mL).

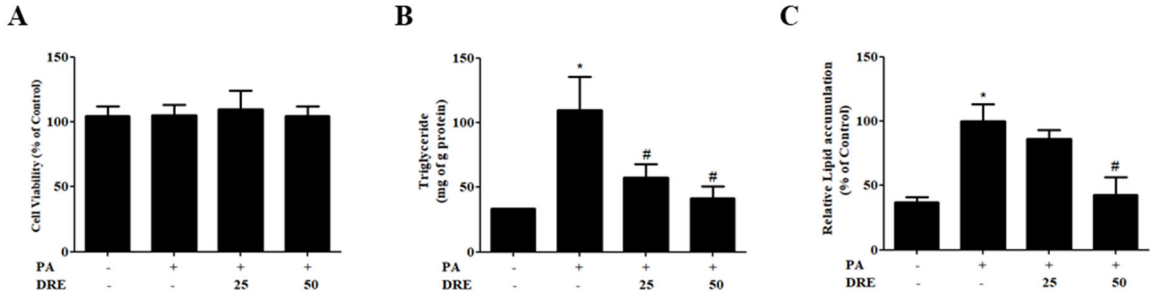


**Figure 1.** Effects of the *Distylium racemosum* ethyl acetate fraction (DRE) on cell viability, triglyceride (TG) levels, and lipid accumulation in palmitic acid (PA)-induced AML12 cells. AML12 hepatocytes were treated with PA (0.5 mM) to induce lipid accumulation and co-treated with DRE at 25 and 50 μg/mL for 24 h. (**A**) Cell viability was assessed using the 3-(4,5-dimethyl-2-thiazolyl)-2,5-diphenyltetrazolium bromide (MTT) assay. No significant cytotoxicity was observed at the tested DRE concentrations. (**B**) Intracellular TG levels were significantly increased by PA (* $p < 0.05$ vs. control). Co-treatment with DRE significantly reduced TG accumulation in a dose-dependent manner (# $p < 0.05$ vs. PA-treated group). (**C**) Oil red O staining revealed markedly increased lipid accumulation in the PA-treated group, but this effect was significantly attenuated by DRE treatment at both concentrations. Data are represented as the mean ± standard deviation (SD). * $p < 0.05$ vs. control group; # $p < 0.05$ vs. PA-treated group.

### *3.2. Effects of DRE on PA-Induced Lipogenesis and Inflammatory Gene Expression Levels in Hepatocytes*

To investigate the effects of DRE on lipogenesis and inflammation following PA treatment, we assessed the expression levels of the related genes. PA significantly increased the expression levels of the lipogenesis-related genes, fatty acid synthase (*FAS*), sterol regulatory element-binding protein 1c (*SREBP1c*), and acetyl-CoA carboxylase (*ACC*). However, DRE decreased the *FAS* and *SREBP1c* levels. *ACC* levels were also decreased, but not significantly, by DRE. Similarly, levels of the inflammatory markers, cluster of differentiation 68 (*CD68*), interleukin-6 (*IL-6*), and monocyte chemoattractant protein-1, were significantly increased by PA but reduced by DRE (Figure 2).

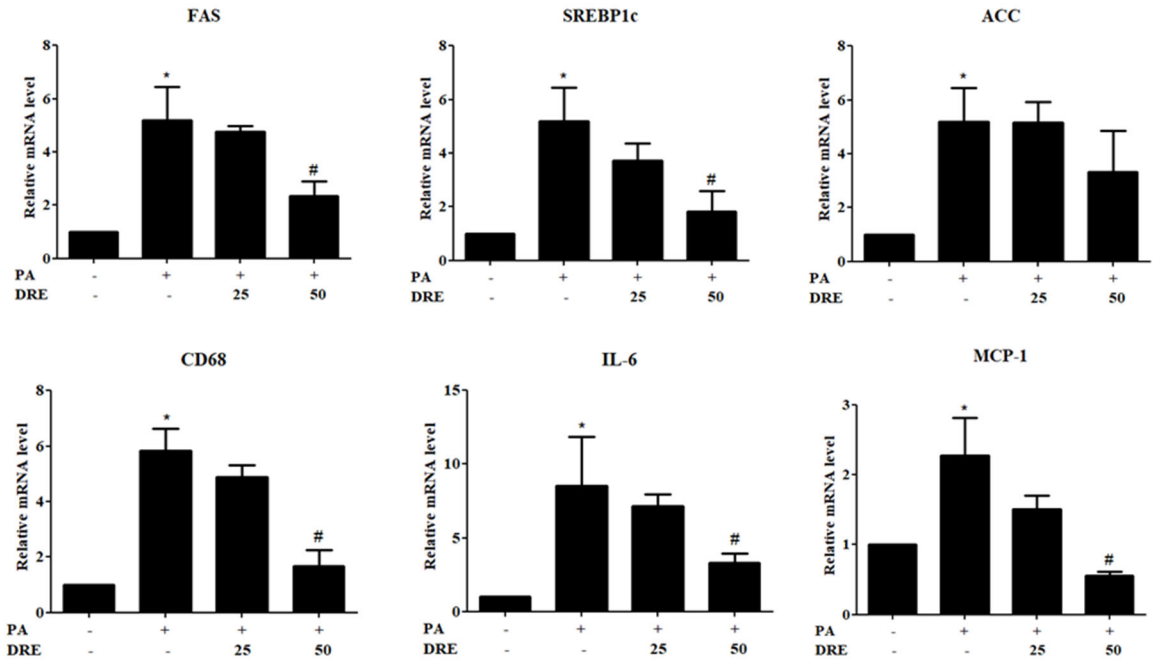


**Figure 2.** Effects of DRE on lipogenic and inflammatory gene expression levels in PA-induced AML12 cells. AML12 cells were treated with PA (0.5 mM) to induce hepatic steatosis and co-treated with DRE at 25 and 50 μg/mL for 24 h. Notably, mRNA expression levels of the lipogenesis-related genes, fatty acid synthase (*FAS*), sterol regulatory element-binding protein 1c (*SREBP1c*), and acetyl-CoA carboxylase (*ACC*), were significantly increased by PA. However, this effect was attenuated by DRE, particularly at 50 μg/mL. Similarly, levels of the inflammatory markers, cluster of differentiation 68 (*CD68*), interleukin-6 (*IL-6*), and monocyte chemoattractant protein-1 (*MCP-1*), were markedly upregulated in the PA-treated group. However, DRE co-treatment significantly reduced their expression levels in a dose-dependent manner. Data are represented as the mean ± SD. * $p < 0.05$ vs. control group; # $p < 0.05$ vs. PA-treated group.

### *3.3. DRE Attenuates Fibrogenic Gene Expression in PA-Induced AML12 Cells*

To assess the antifibrotic effects of DRE, we measured the expression levels of fibrosis-related genes in PA-induced AML12 cells. The following fibrogenic markers were analyzed: collagen type I alpha 1 (*COL1A1*), collagen type I alpha 2 (*COL1A2*), and tissue inhibitor of metalloproteinases 1 (*TIMP1*). PA significantly upregulated the mRNA levels of *COL1A1* and *COL1A2* compared to those in the control group. However, co-treatment with DRE at 50 and 100 μg/mL significantly suppressed this effect in a dose-dependent manner. Although both DRE concentrations reduced the *TIMP1* levels, the changes were not statistically significant (Figure 3).

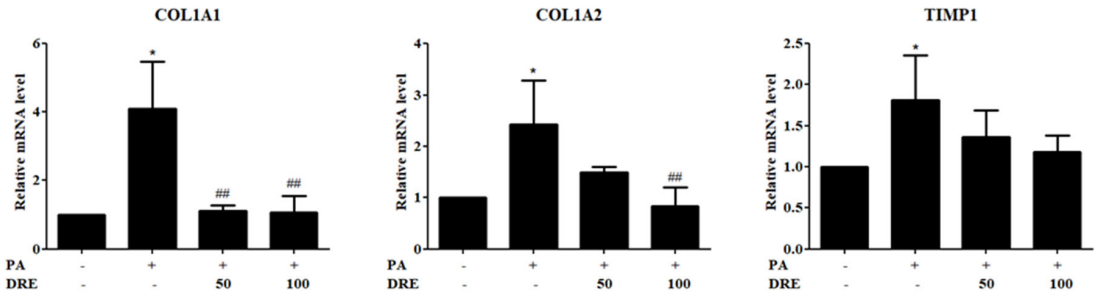


**Figure 3.** Effects of DRE on fibrosis-related gene expression levels in PA-induced AML12 cells. AML12 hepatocytes were treated with PA (0.5 mM) to induce hepatic fibrosis and co-treated with DRE at 50 and 100 μg/mL. Expression levels of the key fibrotic markers, collagen type I alpha 1 (*COL1A1*), collagen type I alpha 2 (*COL1A2*), and tissue inhibitor of metalloproteinases 1 (*TIMP1*), were assessed via quantitative polymerase chain reaction (qPCR). PA significantly upregulated the *COL1A1*, *COL1A2*, and *TIMP1* levels compared to those in the control group (* $p < 0.05$). However, co-treatment with DRE at 50 and 100 μg/mL significantly reduced the *COL1A1* and *COL1A2* levels in a dose-dependent manner (## $p < 0.01$ vs. PA-treated group). Although *TIMP1* levels were also decreased by DRE, no statistical significance was observed.

### *3.4. DRE Reduces the Liver Weight and Improves the Liver Histology in HFMCD Diet-Induced MASH Model Mice*

To evaluate the protective effects of DRE against MASH, we assessed the liver weight, liver-to-body weight ratio, and histopathological changes in the HFMCD diet-induced MASH model mice. HFMCD diet-fed group exhibited significantly higher absolute liver weight and liver-to-body weight ratio than the ND-fed group, indicating that hepatomegaly was associated with steatosis and inflammation. However, DRE significantly reduced liver weight and the liver-to-body weight ratio compared to those in the HFMCD diet-fed group, showing effects comparable to those of quercetin (QUE), an antioxidant flavonoid used as a positive control (Figure 4A,B). Next, histological evaluation of hematoxylin and eosin-stained liver tissues was performed. The ND-fed group showed normal hepatic architecture with no visible lipid accumulation. In contrast, the HFMCD diet-fed group exhibited severe hepatocyte ballooning and excessive accumulation of lipid droplets. Notably, DRE markedly reduced lipid droplet size and accumulation, effectively attenuating hepatic steatosis. Similar histological improvements were observed in the QUE-treated group (Figure 4C).

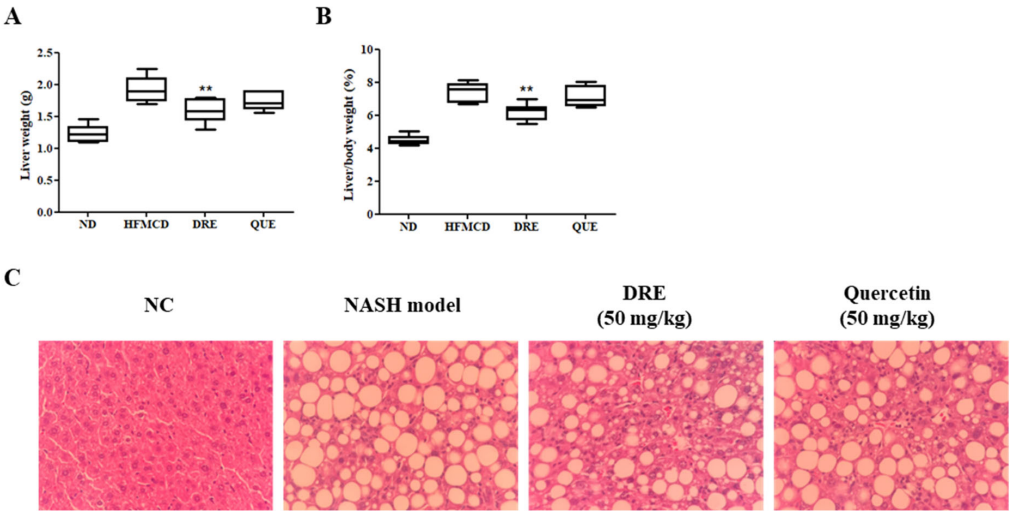


**Figure 4.** Effects of DRE on the liver weight and histological changes in high-fat methionine- and choline-deficient (HFMCD) diet-induced metabolic dysfunction-associated steatohepatitis (MASH)

model mice. The mice were fed an HFMCD diet to induce MASH and subsequently treated with DRE or quercetin (QUE, positive control). A normal diet (ND) group was included as a control. (**A**) Liver weight and (**B**) the liver-to-body weight ratio (%) were significantly increased in the HFMCD diet-fed group compared to those in the ND-fed group. However, DRE significantly reduced liver weight and the liver-to-body weight ratio (** $p < 0.01$ vs. HFMCD diet-fed group), thereby providing hepatoprotection. (**C**) Representative hematoxylin and eosin (H&E)-stained liver sections (original magnification: ×200) showing marked hepatic steatosis and ballooning in the HFMCD diet-fed group. DRE markedly reduced the lipid droplet accumulation, similar to QUE. These results suggest that DRE ameliorates hepatic steatosis and liver hypertrophy in MASH.

### *3.5. DRE Modulates the Gene Expression Levels in HFMCD Diet-Induced MASH Model Mice*

To further elucidate the molecular mechanisms underlying the protective effects of DRE in the liver, we evaluated the mRNA levels of lipid metabolism-, inflammation-, and fibrosis-associated genes in HFMCD diet-induced MASH mouse liver tissues. Levels of peroxisome profiler-activated receptor alpha (PPARα), a major electron factor regulating lipid oxidation, were decreased in the HFMCD diet-fed group compared to those in the ND-fed group. Although DRE slightly increased the PPARα levels, the difference was not statistically significant. Levels of carnitine palmitoyltransferase-1 (CPT-1), a rate-limiting enzyme in mitochondrial fatty acid beta-oxidation, were significantly upregulated in the DRE-treated group compared to those in the HFMCD diet-fed group. In contrast, levels of CD36, an inflammation-related factor, were significantly increased in the HFMCD diet-fed group but significantly reduced by DRE. Similarly, levels of transforming growth factor-β, a fibrosis-related gene, were significantly increased in the HFMCD diet-fed group but significantly downregulated by DRE, suggesting the involvement of DRE in antifibrotic mechanisms. Levels of interleukin-6 (IL-6), a representative inflammatory cytokine, were increased in the HFMCD diet-fed group but reduced by both DRE and QUE, although the changes were not statistically significant (Figure 5).

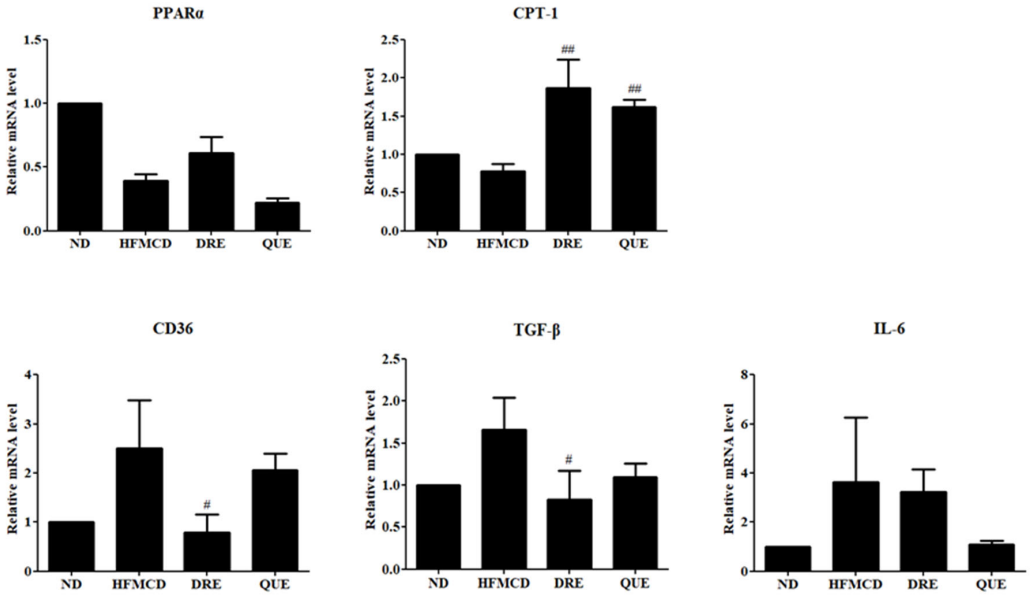


**Figure 5.** Effects of DRE on lipid metabolism, fibrosis, and inflammatory gene expression levels in HFMCD diet-induced MASH model mice. The mice were fed an HFMCD diet to induce MASH and subsequently treated with DRE or QUE (positive control). An ND group was also included as a control. Expression levels of the peroxisome proliferator-activated receptor alpha (PPARα) were reduced in the HFMCD diet-fed group and not significantly restored by either treatment. Levels of carnitine palmitoyltransferase-1 (CPT-1), a key enzyme in mitochondrial fatty acid β-oxidation, were significantly upregulated by both DRE and QUE compared to those in the HFMCD diet-fed

group (## $p < 0.01$). CD36 and transforming growth factor-beta (TGF-β) expression levels were elevated in the HFMCD diet-fed group but significantly reduced by DRE (# $p < 0.05$). Moreover, levels of IL-6, an inflammatory cytokine, were elevated in the HFMCD diet-fed group but subsequently decreased by DRE and QUE in a non-significant manner.

### *3.6. Identification of Rutin in D. racemosum Extracts via HPLC Analysis*

To identify the major bioactive constituents of DRE, HPLC analysis was performed using 18 standard reference compounds, including known flavonoids and phenolic compounds, at a detection wavelength of 360 nm. The chromatographic profile of the standard mixture showed distinct peaks corresponding to the individual compounds, including rutin. A comparison of the chromatograms of the crude extracts of *D. racemosum* and DRE revealed a prominent peak with the same retention time as that of the rutin standard, as indicated by the red marker. However, as shown in the overlaid HPLC chromatograms (Figure 6A), the intensity of the peak corresponding to rutin (retention time: 5.5 min) was relatively low in both the ethanol extract and ethyl acetate fraction of *D. racemosum*, indicating that rutin is a minor component. This identification was based solely on retention time. This confirmed the presence of rutin, which was identified as one of the constituents present in the crude extracts of *D. racemosum* and DRE (Figure 6).

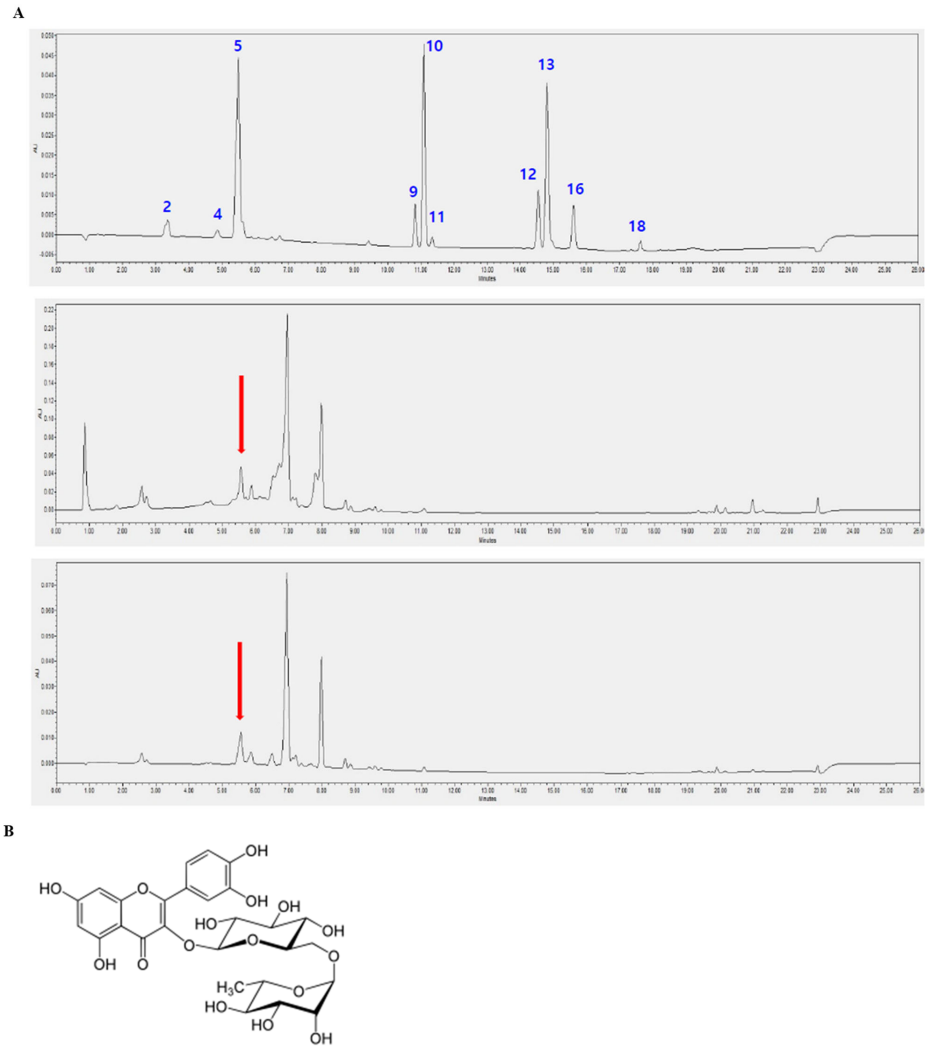


**Figure 6.** Identification of the bioactive compounds in *D. racemosum* extracts via high-performance liquid chromatography (HPLC) analysis. HPLC was performed to identify the bioactive constituents

of the crude extract and DRE using standard compounds. Chromatographic analysis was conducted at 360 nm. (**A**) HPLC chromatograms of (**top**) standard mixture, (**middle**) *D. racemosum* ethanol extract, and (**bottom**) ethyl acetate fraction. The x-axis represents the retention time (minutes), and the y-axis indicates absorbance. The following peaks in the standard mixture are labeled in blue and correspond to the numbered standard compounds: 2: Caffeic acid (3.4 min), 4: p-Coumaric acid (4.8 min), 5: Rutin (5.5 min), 9: Apigenin (10.8 min), 10: Kaempferol (11.0 min), 11: Hesperetin (11.3 min), 12: Chrysin (14.6 min), 13: Acacetin (14.8 min), 16: CAPE (15.6 min), and 18: Artepillin C (17.7 min). The retention time of peak 5 matches that of rutin; however, rutin is only a minor component in both the ethanol extract and DRE. This identification is based solely on retention time. The statement that rutin is a major active component has been revised to reflect that rutin is one of the identified compounds. The red arrows indicate that compound 5 has the same retention time. (**B**) Chemical structure of rutin, a flavonoid compound exhibiting antioxidant, anti-inflammatory, and anti-cancer activities.

## 4. Discussion

Incidence of MASH, a chronic liver disease characterized by hepatic steatosis, inflammation, and fibrosis, steadily increases with obesity and metabolic syndrome [14]. Untreated MASH progresses to cirrhosis and liver cancer, necessitating the development of effective measures for its prevention and treatment [15].

*D. racemosum*, belonging to the *Hamamelidaceae* family, is an evergreen plant species native to East Asia, including Jeju Island in Korea and Japan. Traditionally used for its anti-inflammatory and antioxidant properties, DRE also exerts anti-obesity effects on 3T3-L1 adipocytes in vitro and in high-fat diet-induced obese mouse models in vivo by inhibiting lipid accumulation and body weight gain [10].

As oxidative stress and chronic inflammation caused by excessive lipid accumulation are key pathological features of MASH, natural compounds with antioxidant and anti-inflammatory properties are potential candidates for its prevention and treatment [16]. Based on the previously reported anti-obesity activity of DRE, we hypothesized that its extract protects against MASH. However, specific effects of the *D. racemosum* extract on MASH remain unclear. Therefore, in this study, we investigated the protective effects of DRE in a cellular model of MASH to elucidate its action mechanisms. Our findings provide valuable insights for the development of new therapeutic agents against MASH.

In this study, we demonstrated the hepatoprotective effects of DRE using in vitro and in vivo MASH models. We showed that DRE significantly attenuated lipid accumulation, inflammation, and fibrosis in PA-induced AML12 cells and HFMCD diet-induced MASH model mice. In AML12 hepatocytes, DRE reduced intracellular TG levels and lipid droplet accumulation, as evidenced by oil red O staining. Moreover, DRE downregulated the levels of key lipogenic (FAS, SREBP1c, and ACC) and pro-inflammatory (CD68, IL-6, and monocyte chemoattractant protein-1) genes. These results suggest that DRE exerts anti-lipogenic and anti-inflammatory effects on hepatocytes under lipotoxic conditions.

DRE decreased the fibrotic marker (*COL1A1*, *COL1A2*, and *TIMP1*) levels in PA-treated cells. Additionally, it significantly reduced liver weight and the liver-to-body weight ratio and improved the histological features by decreasing steatosis and hepatocellular ballooning in mice. Metabolic and fibrogenic gene expression levels in liver tissues were determined for the mechanistic analysis of these effects. Indeed, DRE increased the *CPT-1* levels and decreased the *CD36* and transforming growth factor-β levels, exerting potent antifibrotic effects. Although changes in *PPARα* and *IL-6* levels were not statistically significant, the overall expression patterns were consistent with a hepatoprotective profile.

Among the well-studied plant-derived candidates for MASH treatment, QUE and its plant sources exhibit comparable biological activities. For instance, QUE-enriched

extracts of onion peel, Morus alba, and Sophora japonica reduce hepatic steatosis and downregulate the pro-inflammatory cytokine and fibrogenic marker levels in high-fat- and methionine- and choline-deficient-fed rodent models [17–19]. In this study, rutin, a glycosylated derivative of QUE, was identified as the major compound in DRE via HPLC analysis. Rutin shares structural and functional properties with QUE, suggesting potentially equivalent modes of action [20]. This similarity suggests that the hepatoprotective efficacy of DRE is partly attributed to its rutin content.

Silymarin extracted from *Silybum marianum* (milk thistle) is a well-known hepatoprotective agent with antioxidant and antifibrotic activities. Although silymarin strongly suppresses oxidative stress and collagen deposition, it shows limited efficacy in reversing established steatohepatitis [21]. Compared to silymarin, DRE not only reduced fibrogenic marker (*COL1A1*, *COL1A2*, and *TIMP1*) levels but also significantly modulated lipid metabolism by enhancing *CPT-1* levels and reducing *CD36* levels, possibly showing broader action mechanisms.

Resveratrol, a polyphenol found in grapes and berries, exhibits anti-MASH effects by activating the AMP-activated protein kinase and sirtuin 1 pathways and inhibiting adipogenesis [22]. Although further studies are necessary to determine the underlying AMP-activated protein kinase signaling mechanisms, the effects of DRE on SREBP1c and ACC suggest similar regulatory outcomes for adipogenic transcription factors. Moreover, considering its effects on oxidative stress and lipid accumulation, future studies should elucidate the effects and action mechanisms of DRE on lipid metabolism, inflammation, and fibrosis. In conclusion, this study showed that DRE inhibited lipid accumulation, inflammation, and fibrosis, suggesting it as a promising MASH prevention and treatment agent. Furthermore, our findings highlight the value of mechanistic studies based on analysis at the molecular level.

## 5. Conclusions

In this study, we demonstrated that the DRE effectively attenuates key pathological features of MASH, including lipid accumulation, inflammation, and fibrosis, in both hepatocyte and murine models. Application of DRE significantly decreased intracellular triglyceride content and downregulated genes associated with lipid synthesis, inflammation, and fibrosis in palmitic acid-induced AML12 cells. Furthermore, DRE alleviated hepatic steatosis and hepatomegaly in HFMCD-induced MASH model mice, accompanied by modulation of genes involved in lipid metabolism and fibrosis. High-performance liquid chromatography analysis identified rutin as a major active component of DRE, suggesting its potential role in the observed hepatoprotective effects. These results indicate that DRE holds potential as a natural therapeutic option for the management and prevention of MASH and underscore the importance of further studies to elucidate its molecular mechanisms.

**Author Contributions:** Conceptualization, K.-S.C., J.K. and H.-R.K.; methodology, Y.-H.L., M.-H.Y. and W.-J.Y.; software, Y.-H.L. and M.-H.Y.; validation, Y.-H.L. and M.-H.Y.; formal analysis, H.-S.K.; investigation, H.-R.K.; resources, Y.-H.L., M.-H.Y. and W.-J.Y.; data curation, Y.-H.L. and K.-S.C.; writing original draft preparation, Y.-H.L., H.-R.K. and K.-S.C.; writing—review and editing, J.K.; funding acquisition, J.K. and H.-R.K. All authors have read and agreed to the published version of the manuscript.

**Funding:** This research was supported by the National Research Foundation of Korea (NRF) project funded by the Korean government (MSIT) (RS-2022-00165637 to H.-R.K.). This work was supported by the Dongguk University, College of Medicine Research Fund of 2025.

**Institutional Review Board Statement:** The animal study protocol was approved by the Animal Experimentation Ethics Committee of the Catholic University of Pusan (CUP AEC 2023-002).

**Informed Consent Statement:** Not applicable.

**Data Availability Statement:** The original contributions presented in this study are included in the article. Further inquiries can be directed to the corresponding authors.

**Conflicts of Interest:** The authors declare no conflicts of interest.

## Abbreviations

The following abbreviations are used in this manuscript:

| | |
|---|---|
| ACC | Acetyl-CoA carboxylase |
| COL1A1 | Collagen type I alpha 1 |
| CPT-1 | Carnitine palmitoyltransferase-1 |
| DRE | *Distylium racemosum* ethyl acetate fraction |
| FAS | Fatty acid synthase |
| HFMCD | High-fat methionine- and choline-deficient |
| HPLC | High-performance liquid chromatography |
| NAFLD | Non-alcoholic fatty liver disease |
| MASH | Metabolic dysfunction-associated steatohepatitis |
| PA | Palmitic acid |
| SREBP1c | Sterol regulatory element-binding protein 1c |
| TG | Triglyceride |
| TIMP1 | Tissue inhibitor of metalloproteinases 1 |

## References

1. Sheka, A.C.; Adeyi, O.; Thompson, J.; Hameed, B.; Crawford, P.A.; Ikramuddin, S. Nonalcoholic steatohepatitis. *JAMA* **2020**, *323*, 1175–1183. [CrossRef] [PubMed]
2. Abdelmalek, M.F. Nonalcoholic fatty liver disease: Another leap forward. *Nat. Rev. Gastroenterol. Hepatol.* **2021**, *18*, 85–86. [CrossRef]
3. Raza, S.; Rajak, S.; Upadhyay, A.; Tewari, A.; Sinha, R. Current treatment paradigms and emerging therapies for NAFLD/NASH. *Front. Biosci.* **2021**, *26*, 206–237. [CrossRef] [PubMed]
4. Powell, E.E.; Wong, V.W.; Rinella, M. Non-alcoholic fatty liver disease. *Lancet* **2021**, *397*, 2212–2224. [CrossRef] [PubMed]
5. Wei, S.; Wang, L.; Evans, P.C.; Xu, S. NAFLD and NASH: Etiology, targets and emerging therapies. *Drug Discov. Today* **2024**, *29*, 103910. [CrossRef]
6. Friedman, S.L.; Neuschwander-Tetri, B.A.; Rinella, M.; Sanyal, A.J. Mechanisms of NAFLD development and therapeutic strategies. *Nat. Med.* **2018**, *24*, 908–922. [CrossRef]
7. European Association for the Study of the Liver (EASL); European Association for the Study of Diabetes (EASD); European Association for the Study of Obesity (EASO). EASL-EASD-EASO Clinical Practice Guidelines on the management of metabolic dysfunction-associated steatotic liver disease (MASLD). *J. Hepatol.* **2024**, *81*, 492–542. [CrossRef]
8. Huby, T.; Gautier, E.L. Immune cell-mediated features of non-alcoholic steatohepatitis. *Nat. Rev. Immunol.* **2022**, *22*, 429–443. [CrossRef]
9. Huang, Q.; An, Z.; Xin, X.; Gou, X.; Tian, X.; Hu, Y.; Mei, Z.; Feng, Q. The Effectiveness of Curcumin, Resveratrol, and Silymarin on MASLD: A Systematic Review and Meta-Analysis. *Food Sci. Nutr.* **2024**, *12*, 10010–10029. [CrossRef]
10. Kim, H.R.; Jung, B.K.; Yeo, M.H.; Yoon, W.J.; Chang, K.S. Inhibition of lipid accumulation by the ethyl acetate fraction of *Distylium racemosum* in vitro and in vivo. *Toxicol. Rep.* **2019**, *23*, 215–221. [CrossRef]
11. Larsson, S.; Wolk, A. Overweight, obesity and risk of liver cancer: A meta-analysis of cohort studies. *Br. J. Cancer* **2007**, *97*, 1005–1008. [CrossRef] [PubMed]
12. Nagappan, A.; Jung, D.Y.; Kim, J.H.; Lee, H.; Jung, M.H. Gomisin N alleviates ethanol-induced liver injury through ameliorating lipid metabolism and oxidative stress. *Int. J. Mol. Sci.* **2018**, *19*, 2601. [CrossRef] [PubMed]
13. Kim, H.R.; Jung, D.Y.; Kim, S.; Jung, M.H. Preventive effect of poricoic acid against nonalcoholic steatohepatitis. *J. Life Sci.* **2022**, *32*, 962–970.
14. Younossi, Z.M.; Koenig, A.B.; Abdelatif, D.; Fazel, Y.; Henry, L.; Wymer, M. Global epidemiology of nonalcoholic fatty liver disease—Meta-analytic assessment of prevalence, incidence, and outcomes. *Hepatology* **2016**, *64*, 73–84. [CrossRef] [PubMed]

15. Tiniakos, D.G.; Vos, M.B.; Brunt, E.M. Nonalcoholic fatty liver disease: Pathology and pathogenesis. *Annu. Rev. Pathol.* **2010**, *5*, 145–171. [CrossRef]
16. Jadeja, R.; Devkar, R.V.; Nammi, S. Herbal Medicines for the Treatment of Nonalcoholic Steatohepatitis: Current Scenario and Future Prospects. *Evid. Based Complement. Alternat. Med.* **2014**, *2014*, 648308. [CrossRef]
17. Dibal, N.I.; Garba, S.H.; Jacks, T.W. Onion Peel Quercetin Attenuates Ethanol-Induced Liver Injury in Mice by Preventing Oxidative Stress and Steatosis. *Biomed. Res. Ther.* **2022**, *9*, 5102–5112. [CrossRef]
18. Ann, J.Y.; Eo, H.; Lim, Y. Mulberry Leaves (*Morus alba* L.) Ameliorate Obesity-Induced Hepatic Lipogenesis, Fibrosis, and Oxidative Stress in High-Fat Diet-Fed Mice. *Genes Nutr.* **2015**, *10*, 46. [CrossRef]
19. Li, W.; Lu, Y. Hepatoprotective Effects of Sophoricoside against Fructose-Induced Liver Injury via Regulating Lipid Metabolism, Oxidation, and Inflammation in Mice. *J. Food Sci.* **2018**, *83*, 552–558. [CrossRef]
20. Ganeshpurkar, A.; Saluja, A.K. The pharmacological potential of rutin. *Saudi Pharm. J.* **2017**, *25*, 149–164. [CrossRef]
21. Loguercio, C.; Festi, D. Silybin and the liver: From basic research to clinical practice. *World J. Gastroenterol.* **2011**, *17*, 2288–2301. [CrossRef] [PubMed]
22. Wang, S.; Moustaid-Moussa, N.; Chen, L.; Mo, H.; Shastri, A.; Su, R.; Bapat, P.; Kwun, I.; Shen, C.L. Novel insights of dietary polyphenols and obesity. *J. Nutr. Biochem.* **2014**, *25*, 1–18. [CrossRef] [PubMed]